Title

Deep-Layer Microvasculature Dropout by Optical Coherence Tomography Angiography and Microstructure of Parapapillary Atrophy.

Journal

Investigative ophthalmology & visual science, 59(5)

ISSN

0146-0404

Authors

Suh, Min Hee
Zangwill, Linda M
Manalastas, Patricia Isabel C
et al.

Publication Date

2018-04-01

DOI

10.1167/iovs.17-23046

Peer reviewed

Deep-Layer Microvasculature Dropout by Optical Coherence Tomography Angiography and Microstructure of Parapapillary Atrophy

Min Hee Suh,[1] Linda M. Zangwill,[2] Patricia Isabel C. Manalastas,[2] Akram Belghith,[2] Adeleh Yarmohammadi,[2] Tadamichi Akagi,[2,3] Alberto Diniz-Filho,[2] Luke Saunders,[2] and Robert N. Weinreb[2]

[1]Department of Ophthalmology, Haeundae Paik Hospital, Inje University College of Medicine, Busan, South Korea
[2]Hamilton Glaucoma Center, Shiley Eye Institute, the Department of Ophthalmology, University of California San Diego, La Jolla, California, United States
[3]Department of Ophthalmology and Visual Sciences, Kyoto University Graduate School of Medicine, Kyoto, Japan

Correspondence: Robert N. Weinreb, University of California San Diego, 9500 Gilman Drive, MC 0946, La Jolla, CA 92093, USA; rweinreb@ucsd.edu.

Submitted: September 25, 2017
Accepted: March 19, 2018

Citation: Suh MH, Zangwill LM, Manalastas PIC, et al. Deep-layer microvasculature dropout by optical coherence tomography angiography and microstructure of parapapillary atrophy. *Invest Ophthalmol Vis Sci*. 2018;59:1996–2005. https://doi.org/10.1167/iovs.17-23046

Purpose. To investigate the association between the microstructure of β-zone parapapillary atrophy (βPPA) and parapapillary deep-layer microvasculature dropout assessed by optical coherence tomography angiography (OCT-A).

Methods. Thirty-seven eyes with βPPA devoid of the Bruch's membrane (BM) (γPPA) ranging between completely absent and discontinuous BM were matched by severity of the visual field (VF) damage with 37 eyes with fully intact BM (βPPA_{+BM}) based on the spectral-domain (SD) OCT imaging. Parapapillary deep-layer microvasculature dropout was defined as a dropout of the microvasculature within choroid or scleral flange in the βPPA on the OCT-A. The widths of βPPA, γPPA, and βPPA_{+BM} were measured on six radial SD-OCT images. Prevalence of the dropout was compared between eyes with and without γPPA. Logistic regression was performed for evaluating association of the dropout with the width of βPPA, γPPA, and βPPA_{+BM}, and the γPPA presence.

Results. Eyes with γPPA had significantly higher prevalence of the dropout than did those without γPPA (75.7% versus 40.8%; $P = 0.004$). In logistic regression, presence and longer width of the γPPA, worse VF mean deviation, and presence of focal lamina cribrosa defects were significantly associated with the dropout ($P < 0.05$), whereas width of the βPPA and βPPA_{+BM}, axial length, and choroidal thickness were not ($P > 0.10$).

Conclusions. Parapapillary deep-layer microvasculature dropout was associated with the presence and larger width of γPPA, but not with the βPPA_{+BM} width. Presence and width of the exposed scleral flange, rather than the retinal pigmented epithelium atrophy, may be associated with deep-layer microvasculature dropout.

Keywords: deep-layer microvasculature dropout, parapapillary atrophy, optical coherence tomography angiography

β-Zone parapapillary atrophy (βPPA), a feature of the glaucomatous eye,[1] is characterized by atrophy of the retinal pigment epithelium (RPE) and choriocapillaris adjacent to the optic disc.[1–3] It has been suggested that reduced blood supply to the optic nerve head (ONH) due to closure of the choriocapillaris may be a mechanism that accounts for the relationship between the βPPA and glaucoma.[1–5] Specifically, characteristics of the deep-layer microvasculature contained within the βPPA may differ according to whether Bruch's membrane (BM) is present (βPPA_{+BM}), or discontinuous or absent (γ-zone PPA [γPPA]).[3,6–12] In γPPA areas devoid of the BM, parapapillary deep-layer microvasculature is composed of the microvasculature located within the elongated scleral flange.[3,12] In contrast, in βPPA_{+BM} areas, deep-layer microvasculature is only composed of the choriocapillaris.[6,12] However, little is known about this issue since noninvasive visualization of the deep-layer microvasculature has not been possible until the recent development of optical coherence tomography angiography (OCT-A). OCT-A enables visualization of both deep-layer and superficial microvasculature.[6,12–17]

The objective of the present study is to elucidate the association between the microstructure of the βPPA and the deep-layer microvasculature dropout in primary open-angle glaucoma (POAG) patients.

Materials and Methods

POAG patients were included from the Diagnostic Innovations in Glaucoma Study (DIGS) (ClinicalTrials.gov identifier: NCT00221897).[12,15,16,18] Details of the DIGS protocol and eligibility have been described previously.[18] This study was approved by the institutional review boards at the University of California, San Diego, and conformed to the tenets of the Declaration of Helsinki and the Health Insurance Portability and

Accountability Act. Informed consent was obtained from all participants.[12]

Study Subjects

Established POAG patients who had good-quality OCT-A images (Angiovue; Optovue, Inc., Fremont, CA, USA) and radial ONH images using both spectral-domain OCT (SD-OCT) (Spectralis; Heidelberg Engineering GmbH, Heidelberg, Germany) and swept-source OCT (SS-OCT) images (DRI-OCT; Topcon, Tokyo, Japan) were enrolled. All subjects completed an ophthalmologic examination, including assessment of best corrected visual acuity, refractive error, slit-lamp biomicroscopy, intraocular pressure (IOP) measurement with Goldmann applanation tonometry, gonioscopy, central corneal thickness (CCT) measured with ultrasound pachymetry (DGH Technology Inc., Exton, PA, USA), axial length measured by the IOL Master (Carl Zeiss Meditec, Dublin, CA, USA), dilated fundus examination, simultaneous stereophotography of the optic disc, standard automated perimetry (Humphrey Field Analyzer, 24-2 Swedish interactive threshold algorithm; Carl Zeiss Meditec), SD-OCT, OCT-A, and SS-OCT. Perimetry and all imaging tests were conducted within a 6-month period.[12] Systolic and diastolic blood pressure (BP) was measured at the height of the heart with an Omron Automatic BP instrument (Model BP791IT; Omron Healthcare, Inc., Lake Forest, IL, USA). Mean ocular perfusion pressure (MOPP) was calculated according to the following formula: MOPP = ⅔ (mean arterial pressure − IOP), where mean arterial pressure (MAP) = DBP + ⅓ (SBP − DBP). Presence of an optic disc hemorrhage (DH) was defined as an isolated splinter or flame-shaped hemorrhage on the ONH based on standardized review of annually acquired optic disc stereophotographs.[12]

To be included in the current study, POAG patients were required to have visible βPPA on fundus imaging with a temporal width ≥100 μm on at least one radial scan measured by the built-in caliper of the SD-OCT, BVCA ≥20/40, and open angles by gonioscopy.[12] Subjects with a history of ocular intervention (except for uncomplicated cataract or glaucoma surgery), intraocular diseases (e.g., diabetic retinopathy or nonglaucomatous optic neuropathy), or systemic diseases (e.g., stroke or pituitary tumor) that could influence the study results were excluded. Those with systemic hypertension (HT) and diabetes mellitus (DM) were included unless they were diagnosed to have diabetic or hypertensive retinopathy. Subjects with unreliable visual field (VF) or poor-quality imaging tests were also excluded.[12]

POAG was defined as the presence of glaucomatous optic nerve damage (i.e., the presence of focal thinning, notching, localized or diffuse atrophy of retinal nerve fiber layer) and compatible repeated VF damage. Glaucomatous VF damage was defined as a VF outside normal limits on Glaucoma Hemifield Test or pattern standard deviation (PSD) outside 95% normal limits confirmed on two consecutive, reliable (≤20% fixation losses, ≤15% false positives and false negatives) tests.[12]

SD-OCT Imaging of β-Zone Parapapillary Area

Spectralis SD-OCT software (Glaucoma Module Premium Edition, version 1.7.0.0; Heidelberg Engineering GmbH) was used to visualize the ONH, including the PPA area, using a 9×9-mm-sized rectangle centered on the ONH (Fig. 1A1, B1). Details were described elsewhere.[19,20] Briefly, 24 consecutive radial equidistant B-scans were acquired. Each B-scan, subtending 15°, starting from the fovea-BM opening (BMO) axis was automatically determined by the device. From the 24 radial scans, six good-quality radial scans (quality score > 15) extending equidistant from the fovea-BMO axis were selected and included in the analysis (Fig. 1A1).[8]

Analysis of β-Zone Parapapillary Atrophy

The PPA region was evaluated using the Spectralis software feature that facilitated synchronous viewing of the color-converted infrared fundus image and the selected location on the OCT scan.[6–8] The presence of the βPPA was defined as an area without the RPE. γPPA was defined as an area with the exposed Elschnig's ring between the optic disc boundary and the BM tips. Both βPPA and γPPA were required to have a temporal width ≥100 μm on at least one radial OCT scan image as measured by the built-in caliper of the Spectralis OCT (Fig. 1A1, B1).[8,9] The presence of βPPA and γPPA was determined independently by two experienced observers (MHS and PICM) who were masked to patients' clinical information.[8,9] Disagreements were resolved by consensus between the two observers. If consensus could not be reached, the subject was excluded from the analysis.

Eyes with βPPA were divided into two groups according to the presence of γPPA (eyes with and without γPPA). The two groups were matched for the VF mean deviation (MD) to minimize the influence of glaucoma severity on the deep-layer microvasculature dropout.[12,21] Specifically, patients with γPPA were matched to patients without γPPA into three groups based on the severity of their VF damage, (18 early POAG [MD > −6 dB], 12 moderate POAG [−12 dB ≤ MD ≤ −6 dB], and seven advanced POAG [MD < −12 dB]) by using a frequency-matching method. For specific analyses, eyes with γPPA were further classified into two subgroups: (1) those with discontinuous BM (PPA with some BM present) and (2) those lacking BM (PPA in which BM was absent throughout the entire area).[6,8–10] In addition, focal γPPA was defined as γPPA localized to the superior or inferior hemiretina and not involving the fovea-BMO axis (Fig. 1A1).

The βPPA and γPPA width were measured by the two observers (MHS and PICM) as the distance between the temporal optic disc boundary and the temporal margin of the RPE and BM tips, respectively, using the built-in caliper tool of the Spectralis SD-OCT. The average of βPPA and γPPA width measured by the two observers at six radial scans, for which the center was located at the fovea-BMO axis, was calculated (Fig. 1A1, B1).[8] If the temporal margin of the ONH or βPPA was not well visualized, adjacent radial scans 15° apart were used for the measurement. βPPA_{+BM} width was calculated as the difference between the βPPA and γPPA width.

OCT-A Imaging

The Angiovue incorporated in the Avanti SD-OCT system provides noninvasive visualization of the vasculature of various user-defined retinal layers by using the motion contrast technique and split-spectrum amplitude-decorrelation angiography method. Details have been described in elsewhere.[12,13,15–17,22–24] Based on the quality review according to a standard protocol established by the Imaging Data Evaluation and Analysis (IDEA) Reading Center, OCT-A images with poor image quality, as defined by the following criteria, were excluded: (1) a signal strength index <48 (1 = minimum, 100 = maximum), (2) poor clarity, (3) residual motion artifacts visible as irregular vessel pattern or disc boundary on the enface angiogram, (4) local weak signal, (5) segmentation errors of the retinal nerve fiber layer (RNFL) and choroidal layer. The delineation of disc margin was reviewed for accuracy and adjusted manually as necessary according to standard protocols.[12] Vessel density (%) of the microvasculature located in the RNFL was calculated as the proportion of measured area

Investigative Ophthalmology & Visual Science

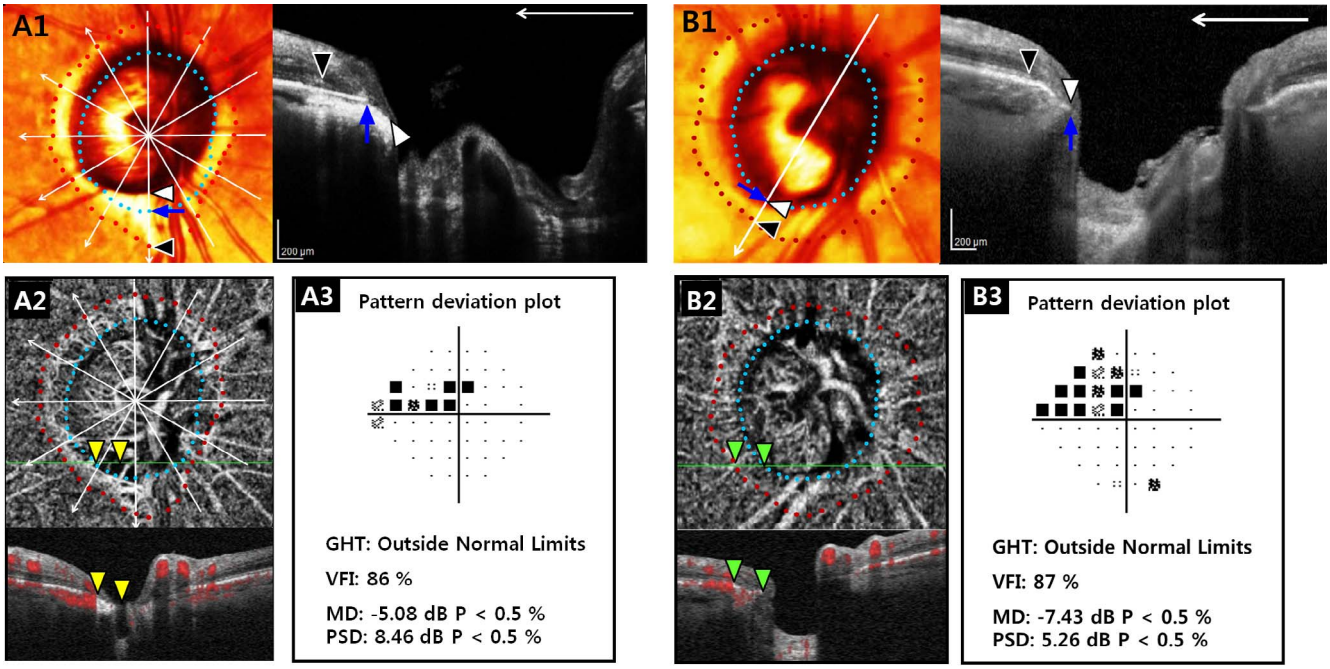

Figure 1. OCT-A–derived deep-layer microvasculature dropout according to the microstructure of βPPA. (**A**) Right eye of 70-year-old POAG patient with βPPA devoid of the BM (γPPA) and (**B**) right eye of 87-year-old POAG patient with βPPA with βPPA_{+BM}, but without γPPA. (**A1**, **B1**) Right images are B-scans obtained at locations indicated by a *white vertical arrow* of the color-converted fundus images. Six radial B-scans (*white arrows*) of the SD-OCT centered on the fovea-BM opening (BMO) axis (*white horizontal arrow*) were selected, and temporal margins of the βPPA_{+BM} indicating RPE tips (*red dots* and *black arrowheads*), γPPA indicating BM termination (*sky blue dots* and *blue arrows*), and optic disc (*white arrowheads*) were delineated. Note that inferior localized γPPA not involving the fovea-BMO axis was present in (**A1**), while βPPA_{+BM} with intact BM occupied the entire βPPA area in (**B1**). (**A2**, **B2**) En face (*upper*) and horizontal (*lower*) B-scans of choroidal layer vessel density maps of the OCT-A. *Green solid lines* indicate locations of B-scans. Well demarcated deep-layer microvasculature dropout (*yellow arrowheads*) within the γPPA was observed in (**A2**), whereas deep-layer microvasculature was relatively preserved (*green arrowheads*) in (**B2**). (**A3**) The two eyes did not show notable difference in the degree of VF damage.

occupied by flowing blood vessels on the ONH 4.5 × 4.5-mm field of view images centered on the optic disc.[12,15,16] Circumpapillary vessel density (cpVD) was calculated in a region defined as a 750-μm-wide elliptical annulus extending from the optic disc boundary based on 360° global area.[12,15,16]

Dropout of the Deep-Layer Microvasculature in the Parapapillary Atrophy

Details for determining the presence of deep-layer microvasculature dropout within the βPPA is described elsewhere.[12] Briefly, two independent observers (MHS and PICM) masked to the patients' baseline characteristics and optic disc features qualitatively analyzed the βPPA area on 4.5 × 4.5-mm-sized choroidal layer vessel density map and the infrared fundus images acquired at the same positions. Discrepancies between the two observers were resolved by consensus, or if consensus could not be reached, the subject was excluded from the analysis.[12] A parapapillary deep-layer microvasculature dropout was defined as a complete loss of the choriocapillaris or the microvasculature within the scleral flange on both horizontal and enface choroidal layer vessel density maps (Fig. 1A2).[12] To avoid false positives, dropout was required to be present in at least four consecutive horizontal scans and also to be ≥200 μm in diameter on at least one scan.[12] To avoid false negatives, reflectance or shadowing of the large vessels on the horizontal and en face images were excluded from the qualitative review.[12] For determining the presence of deep-layer microvasculature dropout within the γPPA in eyes with both dropout and γPPA, Spectralis SD-OCT and OCT-A images were aligned by registering images to large vessels (Fig. 1A1, A2).

SS-OCT Imaging

The optic disc was imaged with the Topcon DRI SS-OCT device to determine the presence of focal lamina cribrosa (LC) defects and to measure choroidal thickness. Details have been described elsewhere.[12,25–27] Both en face and horizontal SS-OCT images covering a 12 × 9-mm cube centered on the posterior pole were obtained using a three-dimensional raster scan (wide-field protocol) consisting of 256 serial horizontal B-scans.[12,25–27]

Poor-quality images with motion artifacts, quality score <50, clipped or poorly focused scans, poorly visible LC, or the segmentation failure of the choroidal layer were excluded.[12,25–27] Poor visibility of the LC was defined as <70% visibility of the anterior laminar surface within the BM opening[12,16] and segmentation failure of choroid as >25% discordance between the visual inspection and the automated identification of the BM and the chorioscleral interface.[12,25,26]

Based on the horizontal and enface SS-OCT images, presence of focal LC defects was determined as laminar holes or laminar disinsertions violating the normal U- or W-shaped contour of the anterior laminar surface by the two observers (MHS and PICM) masked to the patients' clinical information.[12,16,28–34] The subject was excluded from the analysis if consensus between the two observers could not be reached. To be classified as a LC defect, the size of the focal LC defect was required to be ≥100 μm in diameter and >30 μm in depth in at least two consecutive scans.[12,16,28–32] These criteria were

used to reduce the possibility that the LC defects were identified due to the hyporeflective vascular shadowing on the en face SS-OCT images and the disc photographs.[12,16,34]

Total choroidal thickness was derived from the average choroidal thickness values from each of 108 locations from a 1-mm^2-sized grid on the 12 × 9-mm wide-field SS-OCT images using standard SS-OCT software.[12,26]

Data Analysis

Clinical characteristics, ONH morphologic parameters, and OCT-A–derived parameters were compared between eyes with and without γPPA. For continuous variables, Student's *t*-test and Mann-Whitney *U* test were used, depending on the normality test results. For categorical variables, the χ^2 test was performed.[12] Univariable and multivariable logistic regression analyses were performed to determine the association between the parapapillary deep-layer microvasculature dropout and the βPPA microstructure. Variables with a *P* value of <0.10 in the univariable analyses were included in the multivariable logistic regression to adjust potential confounding factors in evaluating association between the deep-layer microvasculature dropout and βPPA microstructure. Interobserver agreement in determining the presence of the βPPA and γPPA, microvasculature dropout, and focal LC defects were assessed using the κ coefficient.[35,36] Interobserver agreement in measuring the βPPA and γPPA width was assessed using Bland-Altman analysis. Statistical software (MedCalc; Med-Calc, Inc., Mariakerke, Belgium) was used for statistical analyses, and the α level (type I error) was set at 0.05.

Results

Study Population

One hundred forty eyes of 140 consecutive POAG DIGS patients who were evaluated for eligibility were included in this report. Of these 140 eyes, 27 were excluded for the following reasons: (1) poor-quality SD-OCT images ($n = 9$), (2) an absence of βPPA ($n = 11$), and (3) temporal βPPA width <100 mm ($n = 7$). Among the remaining 113 eyes of 113 patients, 11 eyes were excluded due to poor OCT-A, nine eyes due to poor SS-OCT images, and one eye due to failure to reach the consensus between observers for the determination of the deep-layer microvasculature dropout. A final sample of 92 eyes was available for analysis; from this sample, 37 eyes with γPPA were matched for severity of VF damage by the frequency-matching method with 37 eyes without γPPA. Six of 37 eyes (16.2%) had γPPA lacking BM, whereas the remaining 31 eyes (83.8%) had discontinuous BM.

Clinical characteristics and presence of the deep-layer microvasculature dropout of the POAG patients (37 with and 37 without γPPA) were compared (Table 1). Eyes with and without γPPA were not significantly different with respect to sex; CCT; ethnicity; presence of diabetes and systemic hypertension; antihypertensive and diabetes medication; number of glaucoma medications; IOP; systolic and diastolic BP MOPP; presence of the DH, VF MD, VF PSD; presence of the focal LC defect; and total choroidal thickness (all $P > 0.10$). Eyes with γPPA were more myopic and had longer axial lengths than those without γPPA (–2.4 ± 2.5 vs. –0.5 ± 1.6 diopter [D] for spherical equivalent and 25.2 ± 1.4 vs. 24.0 ± 1.0 mm for axial length; $P < 0.05$). Subjects who had eyes with γPPA were younger than those without γPPA with marginal significance (70.0 ± 10.9 vs. 74.8 ± 11.9 years; $P = 0.073$). Upper nasal and inferonasal cpVD were significantly higher (54.1% ± 6.1% versus 50.2% ± 9.3% for upper nasal cpVD and 55.4% ± 10.1% versus 50.2% ± 9.3% for inferonasal cpVD; $P < 0.05$) in eyes with γPPA compared to eyes without γPPA. For all other RNFL and cpVD variables, the two groups were not different (all $P > 0.10$).

Interobserver Agreement for the Measurement

Interobserver agreement for determining the γPPA, γPPA with discontinuous BM, focal γPPA, deep-layer microvasculature dropout, and focal LC defect were excellent (κ = 0.86, 95% confidence interval [CI] 0.75–0.98, $P < 0.001$ for γPPA; κ = 0.89, 95% CI 0.69–1.00, $P < 0.001$ for γPPA with discontinuous BM; κ = 0.87, 95% CI 0.63–1.00, $P < 0.001$ for focal γPPA; κ = 0.86, 95% CI 0.74–0.98, $P < 0.001$ for dropout; and κ = 0.82, 95% CI 0.70–0.94, $P < 0.001$ for focal LC defect).[36] Based on the Bland-Altman plot, there was good agreement between the two observers in the βPPA and γPPA width as follows: the mean differences between the two observers were 21.5 μm (95% CI, 4.4–38.6 μm) for βPPA width and 42.3 μm (95% CI, 21.2–63.4 μm) for γPPA width, respectively; the 95% CI of the limits of agreement for βPPA width was –123.3 to 166.3 μm (95% CI of the upper limits, 136.9–195.6 μm; lower limits, –152.6 to –93.9 μm), and for γPPA width was –81.6 to 166.2 μm (95% CI of the upper limits, 129.9–202.6 μm; lower limits, –118.0 to –45.3 μm) (Fig. 2).

Deep-Layer Microvasculature Dropout and ONH Morphologic Parameters in Eyes With and Without γPPA

The ONH morphologic parameters measured by Spectralis SD-OCT and presence of the parapapillary deep-layer microvasculature dropout were compared between eyes with and without γPPA (Table 2). Eyes with γPPA had a significantly higher prevalence of the deep-layer microvasculature dropout (75.7% versus 40.8%; $P = 0.004$), larger βPPA width (411.4 ± 211.5 vs. 277.4 ± 97.8 μm; $P < 0.001$), and smaller βPPA_{+BM} width (180.3 ± 120.1 vs. 277.4 ± 97.8 μm; $P < 0.001$). The two groups were not significantly different with respect to the BMO area ($P = 0.947$) and fovea-BMO angle ($P = 0.900$). Among 28 eyes with both γPPA and deep-layer microvasculature dropout, 26 eyes (92.9%) had γPPA areas containing dropouts (Fig. 1A1).

βPPA Microstructure and Deep-Layer Microvasculature Dropout

Univariable and multivariable logistic regression analyses were used to evaluate the association between the width of βPPA, γPPA, and βPPA_{+BM} and presence of the γPPA and parapapillary deep-layer microvasculature dropout (Tables 3–6).

In the univariable analysis (Table 3), parapapillary deep-layer microvasculature dropout was significantly associated with the longer βPPA width (odds ratio [OR], 1.01; $P = 0.0008$), γPPA presence (OR, 4.08; $P = 0.004$), longer γPPA width (OR, 1.01; $P = 0.0052$), lower cpVD (OR, 1.16; $P < 0.001$), worse VF MD (OR, 1.24; $P < 0.001$), presence of the focal LC defect (OR, 3.18; $P = 0.017$), thinner total choroidal thickness (OR, 1.01; $P = 0.025$), and longer axial length (OR, 1.49; $P = 0.036$). Age; sex; race; CCT; IOP; systolic and diastolic BP; MOPP; prevalence of the DM, HT, and DH; BMO opening area; fovea-BMO angle; and βPPA_{+BM} width were not significantly associated with microvasculature dropout (all $P > 0.10$).

Table 1. Comparison of the Demographics and Test Results Between POAG Patients According to the Presence of the βPPA Devoid of the BM (γPPA)

Variables	Eyes With γPPA, 37 Eyes, 37 Patients	Eyes Without γPPA, 37 Eyes, 37 Patients	*P* Value
Age, y	70.0 ± 10.9	74.8 ± 11.9	0.073*
Sex, male/female	18/19	20/17	0.816†
Spherical equivalent, D	−2.4 ± 2.5	−0.5 ± 1.6	**<0.001***
Axial length, mm	25.2 ± 1.3	24.0 ± 1.0	**<0.001***
CCT, μm	534.8 ± 55.4	530.7 ± 40.9	0.720*
Ethnicity, Asian/European/African descent	6/28/3	4/24/9	0.157†
Self-reported history of diabetes, *n* (%)	0 (0)	4 (10.8)	0.123†
Self-reported history of hypertension, *n* (%)	12 (32.4)	18 (48.6)	0.163†
Antihypertensive medication, *n* (%)	10 (27.0)	14 (37.8)	0.456†
Diabetes medication, *n* (%)	0 (0)	3 (8.1)	0.239†
Topical glaucoma medications, *n*			0.225†
0	8	14	
1	17	16	
>1	12	7	
Topical medications, *n*			0.360†
Prostaglandin analogues	23	20	
β-antagonists	10	3	
Carbonic anhydrase inhibitors	10	4	
α-1 agonist	6	5	
IOP, mm Hg	14.5 ± 4.5	13.3 ± 5.0	0.179‡
Systolic BP, mm Hg	122.0 ± 15.0	130.2 ± 12.5	**0.027**‡
Diastolic BP, mm Hg	75.9 ± 9.8	77.4 ± 11.2	0.546*
MOPP, mm Hg	61.5 ± 13.1	59.6 ± 11.2	0.499‡
DH, *n* (%)	9 (24.3)	3 (8.1)	0.115†
VF MD, dB	−7.47 ± 5.97	−7.92 ± 7.00	0.974‡
VF PSD, dB	7.95 ± 4.23	6.45 ± 4.02	0.144‡
cpRNFL thickness, μm			
Global area	69.8 ± 11.0	69.3 ± 11.6	0.828*
Upper temporal	58.4 ± 15.6	57.3 ± 13.4	0.746*
Upper nasal	64.3 ± 11.3	60.3 ± 13.4	0.164*
Lower nasal	59.1 ± 9.9	57.0 ± 10.3	0.380*
Lower temporal	51.3 ± 11.7	53.4 ± 9.4	0.393*
Superotemporal	93.4 ± 22.7	88.8 ± 18.4	0.341*
Superonasal	82.7 ± 16.9	77.2 ± 17.2	0.167*
Inferonasal	75.1 ± 17.5	77.7 ± 20.9	0.566*
Inferotemporal	74.7 ± 23.3	82.5 ± 24.0	0.163*
Whole-image vessel density, %	46.5 ± 5.3	45.0 ± 5.5	0.226*
Circumpapillary vessel density, %			
Global area	54.0 ± 6.2	53.0 ± 6.6	0.514*
Upper temporal	58.8 ± 9.7	58.1 ± 8.3	0.556‡
Upper nasal	54.1 ± 6.1	50.2 ± 9.3	**0.013***
Lower nasal	52.1 ± 6.7	51.6 ± 7.4	0.756*
Lower temporal	55.9 ± 8.4	55.5 ± 7.2	0.810*
Superotemporal	55.6 ± 9.6	53.6 ± 8.8	0.365*
Superonasal	54.8 ± 6.1	52.3 ± 7.3	0.107*
Inferonasal	55.4 ± 10.1	50.2 ± 9.3	**0.024***
Inferotemporal	48.6 ± 10.5	52.4 ± 11.1	0.133*
Focal LC defect, *n* (%)	18 (48.6)	19 (51.4)	0.829*
Total choroidal thickness, μm	137.1 ± 45.9	159.9 ± 64.7	0.158‡

Values are shown in mean ± standard deviation. Statistically significant values are shown in bold. D, diopter; cpRNFL, circumpapillary retinal nerve fiber layer.

* The comparison was performed using independent samples *t*-test.

† The comparison was performed using χ^2 test.

‡ The comparison was performed using Mann-Whitney *U* test.

In order to avoid issues of multicollinearity in the multivariable analysis, we evaluated the correlations between covariates. We found that VF MD, cpVD, and presence of the focal LC defects were significantly associated with one another. For this reason, the correlated variables were included in the multivariable model separately to avoid issues of multicollinearity.

γPPA Presence and Deep-Layer Microvasculature Dropout

Multivariable logistic regression analysis demonstrated that γPPA presence remained as a significant factor associated with the presence of dropout after adjusting for axial length, total choroidal thickness, and VF MD (OR, 5.34; $P = 0.012$) (Table

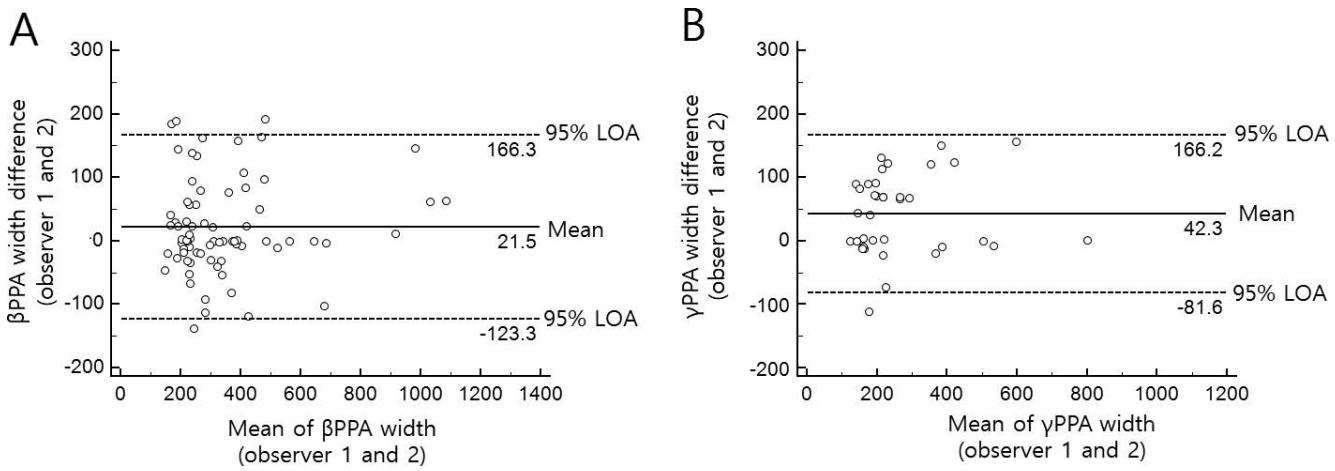

Figure 2. Bland-Altman plots showing the width of βPPA (**A**) and γPPA (**B**) of the two observers. The *solid lines* represent the mean difference, and the *dashed lines* represent the 95% limits of agreement (LOA).

4). Similarly, γPPA presence remained as a significant factor associated with deep-layer microvasculature dropout in models when focal LC defects (OR, 3.75; $P = 0.030$) and cpVD (OR, 5.67; $P = 0.009$) each were included in the multivariable models instead of VF MD (Table 4).

γPPA Width and Deep-Layer Microvasculature Dropout

Longer γPPA width also remained as a significant factor associated with deep-layer microvasculature dropout after adjusting axial length, total choroidal thickness, and VF MD (OR, 1.01; $P = 0.039$) (Table 5). Similar patterns were observed in the multivariable analysis when cpVD was included instead of VF MD (OR, 1.01; $P = 0.048$). When focal LC defect was included instead of VF MD, γPPA width was marginally significant (OR, 1.01; $P = 0.073$) (Table 5).

Focal γPPA and Deep-Layer Microvasculature Dropout

Five of 37 eyes (13.5%) with γPPA had focal γPPA not involving the fovea-BMO axis, and all of them had deep-layer microvasculature dropout located within the γPPA region (Fig. 1A1).

Table 2. Comparison of the ONH Morphologic Parameters Measured by Spectralis SD-OCT and Presence of the Parapapillary Deep-Layer Microvasculature Dropout Measured by OCT-A Between Eyes With and Without γPPA According to the Presence of the βPPA Devoid of the BM

Variables	Eyes With γPPA, 37 Eyes, 37 Patients	Eyes Without γPPA, 37 Eyes, 37 Patients	*P* Value
BMO area, mm^2	2.1 ± 0.6	2.1 ± 0.5	0.947*
Fovea-BMO angle, deg	−7.6 ± 3.9	−7.7 ± 4.6	0.900*
βPPA width, μm	411.4 ± 211.5	277.4 ± 97.8	**<0.001**†
$βPPA_{+BM}$ width, μm	180.3 ± 120.1	277.4 ± 97.8	**<0.001**†
Presence of the deep-layer microvasculature dropout, %	28 (75.7)	15 (40.8)	**0.004**‡

* The comparison was performed by using independent samples *t*-test.

† The comparison was performed by using Mann-Whitney *U* test.

‡ The comparison was performed by using χ^2 test.

Eyes with focal γPPA had significantly shorter axial length than the remaining 32 eyes with γPPA involving the fovea-BMO axis (23.7 ± 0.80 vs. 25.5 ± 1.3 mm, $P = 0.005$; independent *t*-test).

βPPA Width and Deep-Layer Microvasculature Dropout

βPPA width was not significantly associated with the deep-layer microvasculature dropout after adjusting for axial length, total choroidal thickness, and VF MD ($P = 0.176$) (Table 6). Similar patterns were observed in the multivariable analysis when focal LC defect ($P = 0.112$) and cpVD ($P = 0.166$) were included instead of VF MD (Table 6). In all multivariable logistic regression analyses, worse VF MD was significantly associated with the deep-layer microvasculature dropout (all $P < 0.05$), while axial length and total choroidal thickness were not significantly associated with the dropout (all $P > 0.10$) (Tables 4–6).

Discussion

This study found that glaucomatous eyes with γPPA had a significantly higher prevalence of parapapillary deep-layer microvasculature dropout than those with $βPPA_{+BM}$ (75.7% versus 40.8%, $P = 0.004$; χ^2 test). Furthermore, parapapillary deep-layer microvasculature dropout was positively associated with the presence and longer width of the γPPA even after adjusting for other potentially confounding factors such as axial length, choroidal thickness, glaucoma severity, and presence of focal LC defects.[12] However, width of the $βPPA_{+BM}$ was not associated with deep-layer microvasculature dropout. These findings suggest that parapapillary deep-layer microvasculature dropout may be associated with a continuum of γPPA with exposed scleral flange ranging from completely present to completely absent but not with the area of $βPPA_{+BM}$ with atrophic change of the RPE.

Our previous study[12] showed that deep-layer microvasculature dropout within the βPPA was associated with more advanced disease status, presence of a focal LC defect, reduced superficial microvasculature, thinner choroidal thickness, and lower diastolic BP. However, in the previous study, the association between the dropout and microstructure of βPPA was not evaluated.[12] The current study demonstrated that γPPA area was significantly associated with the presence of deep-layer microvasculature dropout. These results are consis-

Table 3. Univariate Logistic Regression Evaluating Factors Associated With the Presence of Parapapillary Deep-Layer Microvasculature Dropout ($n = 74$)

	Univariate Model	
Variables	**Odds Ratio, 95% CI**	***P* Value**
Age, per 1 y older	1.02, 0.98–1.06	0.418
Female vs. male	2.17, 0.84–5.58	0.106
Non-white race vs. white	1.33, 0.49–3.65	0.577
CCT, per 1 μm thinner	1.01, 1.00–1.02	0.260
IOP, per 1 mm Hg lower	1.09, 0.98–1.20	0.109
Systolic BP, per 1 mm Hg higher	1.00, 0.97–1.04	0.782
Diastolic BP, per 1 mm Hg lower	1.04, 0.99–1.09	0.113
MOPP, per 1 mm Hg higher	1.02, 0.98–1.06	0.375
Diabetes, absence	1.50, 0.19–0.20	0.695
Hypertension, absence	1.21, 0.47–3.12	0.687
DH, absence	1.06, 0.30–3.71	0.931
Circumpapillary vessel density, per 1% lower	1.16, 1.05–1.28	**<0.001**
VF MD, per 1 dB worse	1.24, 1.09–1.42	**<0.001**
Focal LC defect, detection	3.18, 1.22–8.39	**0.017**
Total choroidal thickness, per 1 μm thinner	1.01, 1.00–1.02	**0.025**
Axial length, per 1 mm longer	1.49, 1.00–2.21	**0.036**
BMO opening area, per 1 mm^2 larger	1.53, 0.54–4.29	0.421
Fovea-BMO angle	0.99, 0.89–1.11	0.898
βPPA width, per 1 μm larger	1.01, 1.00–1.01	**<0.001**
$βPPA_{+BM}$ width, per 1μm larger	1.00, 1.00–1.00	0.714
γPPA, presence	4.08, 1.51–11.03	**0.004**
γPPA width, per 1 μm larger	1.01, 1.00–1.01	**0.005**

Statistically significant values are shown in bold. $βPPA_{+BM}$, γPPA.

tent with previous studies suggesting that penetrating branches of the short posterior ciliary artery passing through the scleral flange may be subject to increased mechanical stress and strain.[37,38] Therefore, γPPA with exposed scleral flange may be a sign of increased IOP-related scleral tension that leads to disruption of the deep-layer microvasculature. Further measurement of the IOP-related stress or strain and subsequent vascular changes according to the presence and continuum of the exposed scleral flange are warranted to elucidate this speculation.

However, how the relationship between the γPPA and parapapillary deep-layer microvasculature dropout relates to the pathophysiology of glaucoma is still unclear. The current results do not concur with other studies suggesting that the presence and width of the γPPA may be associated with slower progression of glaucoma[9,10] and with studies suggesting that deep-layer microvasculature dropout is associated with a more advanced disease status.[11,12] Also, the presence and width of the γPPA is known to be associated with axial elongation of the eye globe.[6,7] Therefore, as axial globe elongation is halted with aging, the mechanical stress due to scleral stretching may also be relieved. Possible explanations for the discrepancies among studies may be attributed to differences of the study population and definition regarding the microstructure of the PPA.[6,7] In the current study, glaucomatous eyes with γPPA had significantly longer axial lengths, larger βPPA width, and smaller BMO area than those without γPPA. In a univariable regression for determining factors associated with the deep-layer microvasculature dropout, axial length and βPPA width remained as associated factors as well as the presence and width of γPPA. However, in multivariable regression, only the width and presence of the γPPA were significantly associated with deep-layer microvasculature dropout; axial length and βPPA width, therefore, were excluded in most models. One possible explanation for these results is a relatively small number of eyes with high myopia (axial length $\geq$ 26.5 mm or spherical equivalent $\geq$ –6.0 D) ($n = 7$) and older patients with γPPA (72.4 years) than those of previous studies (age ranging between 42.9 and 58.9 years).[6,9,10] Therefore, there were proportionately fewer γPPA eyes that completely lacked BM (16.2%, $n = 6$) than in previous studies (percentage of γPPA completely lacking BM ranging between 18.8% and 35.6%).[6,9,10] Second, a pathogenic process other than axial elongation may contribute to the development of a certain type of βPPA devoid of BM and vascular disruption. In this study, five (13.5%) of 37 eyes with γPPA had focal γPPA that does not involve the fovea-BMO axis, and their axial length was shorter than that of the remaining 32 eyes with γPPA involving the fovea-BMO axis (23.7 vs. 25.5 mm, $P = 0.005$; independent *t*-test). In addition, eyes with focal γPPA in our study have relatively shorter axial lengths (mean = 23.7 mm) than those with γPPA in previous studies (mean axial length ranging between 25.74 and 26.42 mm).[6,9,10] It is interesting that all eyes with focal γPPA had deep-layer microvasculature dropout. Given that axial growth of the globe leads to the temporal dragging of the ONH,[39] it is less likely that γPPA induced by axial elongation does not involve the fovea-BMO axis, a central horizontal axis of the ONH. Therefore, focal γPPA not involving the fovea-BMO axis may reflect a local alteration of the BM and loss of an adjacent deep-layer microvasculature derived by mechanisms other than those from axial elongation. However, the role of focal γPPA and its relationship with the deep-layer microvasculature disruption in the pathophysiology of glaucoma can only be confirmed by future studies with a larger

Table 4. Multivariate Logistic Regression Testing the Association Between the Parapapillary Deep-Layer Microvasculature Dropout and the Presence of βPPA Devoid of the BM (γPPA) ($n = 74$)

	Multivariate Model 1 With VF MD, AXL, and CT Included		Multivariate Model 2 With Focal LC Defect, AXL, and CT Included		Multivariate Model 3 With cpVD, AXL, and CT Included	
Variables	**Odds Ratio, 95% CI**	***P* Value**	**Odds Ratio, 95% CI**	***P* Value**	**Odds Ratio, 95% CI**	***P* Value**
γPPA, presence	5.34, 1.46–19.57	**0.012**	3.75, 1.14–12.33	**0.030**	5.67, 1.53–20.98	**0.009**
AXL, per 1 mm longer	1.04, 0.61–1.80	0.877	1.17, 0.70–1.94	0.544	1.09, 0.64–1.85	0.752
CT, per 1 μm thinner	1.01, 1.00–1.02	0.175	1.01, 1.00–1.02	0.228	1.01, 1.00–1.02	0.218
VF MD, per 1 dB worse	1.28, 1.10–1.49	**0.001**				
Focal LC defect, presence			3.67, 1.23–10.96	**0.020**		
cpVD, per 1% lower					1.20, 1.08–1.35	**0.001**

Statistically significant values are shown in bold. AXL, axial length; CT, total choroidal thickness.

Investigative Ophthalmology & Visual Science

Table 5. Multivariate Logistic Regression Testing the Association Between the Parapapillary Deep-Layer Microvasculature Dropout and the Width of βPPA Devoid of the BM (γPPA) ($n = 74$)

	Multivariate Model 1 With VF MD, AXL, and CT Included		Multivariate Model 2 With Focal LC Defect, AXL, and CT Included		Multivariate Model 3 With cpVD, AXL, and CT Included	
Variables	Odds Ratio, 95% CI	*P* Value	Odds Ratio, 95% CI	*P* Value	Odds Ratio, 95%CI	*P* Value
γPPA width, 1 μm larger	1.01, 1.00–1.01	**0.039**	1.01, 1.00–1.01	0.073	1.01, 1.00–1.01	**0.048**
AXL, per 1 mm longer	0.97, 0.55–1.72	0.923	1.10, 0.64–1.88	0.741	1.04, 0.55–1.67	0.878
CT, per 1 μm thinner	1.01, 1.00–1.02	0.150	1.01, 1.00–1.02	0.202	1.01, 1.00–1.02	0.154
VF MD, per 1 dB worse	1.29, 1.10–1.49	**0.002**				
Focal LC defect, presence			3.34, 1.15–9.73	**0.027**		
cpVD, per 1% lower					1.18, 1.06–1.32	**0.003**

Statistically significant values are shown in bold.

number of study subjects with focal γPPA. Further longitudinal studies with larger numbers of normal and glaucomatous eyes with high myopia are required to determine whether the rate of glaucoma progression differs according to the axial length, type of γPPA, and the presence of deep-layer microvasculature dropout.

The current finding that βPPA width was associated with the deep-layer microvasculature dropout in univariable regression analysis, but not in multivariable regression analysis, concurs with our previous results.[12] Furthermore, βPPA_{+BM} width was not associated with dropout in univariable regression analysis. However, these results do not correspond with previous histologic studies showing that age-related atrophy of the RPE-BM complex, known to be a main mechanism of the βPPA_{+BM}, was associated with the complete loss of adjacent choriocapillaris.[3,40] Differences across the studies may be related to differences in study design. The present study utilized an in vivo imaging device, whereas previous studies used histopathologic analysis. Technical limits of the current OCT-A device and qualitative analysis of the deep-layer microvasculature dropout may also hinder detection of the subtle loss of parapapillary deep-layer microvasculature in this study.[12] Further improvement of the OCT-A technique and quantitative analysis of the deep-layer microvasculature is needed.

Despite controversy over the relationship between the choroidal thickness and deep-layer microvasculature dropout,[12,17] the current result concurs with a recently published study that choroidal thickness is not related to the presence of the deep-layer microvasculature dropout.[17] Considering their topographical relationship, it will be important to investigate the association between the parapapillary deep-layer microvasculature and the adjacent choroidal structure outside the PPA.

The present study has several limitations. First, eyes with and without γPPA were matched by the severity of glaucoma to minimize the possibility of selection bias that more severe glaucoma eyes are more likely to have deep-layer microvasculature dropout. Therefore, caution is needed in interpreting the study results that γPPA was associated with microvasculature dropout. However, matching did have an advantage as it made for a more controlled experiment since both deep-layer microvasculature dropout and presence of the γPPA were known to be associated with the glaucomatous severity.[9–12] Future studies with larger numbers of glaucomatous eyes with typical γPPA completely devoid of BM are warranted. Second, as three devices were used for determining the presence of γPPA in this study, variability of registration across images may have reduced the strength of the associations. Spectralis SD-OCT and SS-OCT, instruments that enabled good visualization of the deeper layers, were utilized to visualize the RPE and BMO tips, choroidal tissue, and presence of focal LC defects, whereas Avanti OCT-A was utilized to assess deep-layer microvasculature.[12] However, the three devices were aligned by using large retinal vessels for determining the location of dropout within the γPPA, thereby reducing the likelihood of large misalignment between images.[16] Third, it is still unclear whether optic disc margin based on the infrared fundus image may reflect an anatomically correct structure, since disc margin does not uniformly correspond to the BMO-based disc margin of SD-OCT images.[6,9,19,20,41] This may limit an accurate determination of the RPE and BM and thus may lead to a variation in the measurement of the βPPA, γPPA, and βPPA_{+BM} width. However, interobserver agreement for measurement of

Table 6. Multivariate Logistic Regression Testing the Association Between the Parapapillary Deep-Layer Microvasculature Dropout and βPPA Width ($n = 74$)

	Multivariate Model 1 With VF MD, AXL, and CT included		Multivariate Model 2 With Focal LC Defect, AXL, and CT Included		Multivariate Model 3 With cpVD, AXL, and CT Included	
Variables	Odds Ratio, 95% CI	*P* Value	Odds Ratio, 95% CI	*P* Value	Odds Ratio, 95% CI	*P* Value
βPPA width, per 1 mm larger	1.00, 1.00–1.01	0.176	1.00, 1.00–1.01	0.112	1.00, 1.00–1.01	0.166
AXL, per 1 mm longer	1.25, 0.76–2.03	0.380	1.27, 0.79–2.06	0.323	1.28, 0.78–2.10	0.323
CT, per 1 μm thinner	1.01, 1.00–1.02	0.212	1.01, 1.00–1.02	0.313	1.01, 1.00–1.02	0.233
VF MD, per 1 dB worse	1.24, 1.08–1.43	**0.002**				
Focal LC defect, presence			3.15, 1.09–9.05	**0.033**		
cpVD, per 1% lower					1.16, 1.04–1.29	**0.006**

Statistically significant values are shown in bold.

Investigative Ophthalmology & Visual Science

the βPPA and γPPA width was good (Fig. 2), and adjunct usage of the infrared fundus images synchronous to the SD-OCT also helped to accurately determine the RPE and BMO tips.

In conclusion, parapapillary deep-layer microvasculature dropout was significantly associated with the presence and larger width of the βPPA without BM (γPPA) in glaucomatous eyes, but not with the width of βPPA with intact BM. These findings suggest that the increased strain and stress on the exposed scleral flange without BM rather than atrophic change of the RPE may be associated with the complete loss of parapapillary deep-layer microvasculature. How this relationship between the mechanical and vascular parameters of the ONH affects the pathophysiology of the development and progression of glaucoma remains to be elucidated.

Acknowledgments

Supported in part by National Institutes of Health/National Eye Institute Grants P30EY022589, EY11008, EY019869, EY021818, and an unrestricted grant from Research to Prevent Blindness (New York, NY, USA) and the donors of the National Glaucoma Research, a BrightFocus Foundation. The funding organizations had no role in the design or conduct of this research.

Disclosure: **M.H. Suh**, None; **L.M. Zangwill**, Carl Zeiss Meditec (F), Heidelberg Engineering (F), Merck (C), National Eye Institute (F), Optovue (F), Topcon (F); **P.I.C. Manalastas**, None; **A. Belghith**, None; **A. Yarmohammadi**, None; **T. Akagi**, None; **A. Diniz-Filho**, None; **L. Saunders**, None; **R.N. Weinreb**, Alcon (C), Allergan (C), Bausch & Lomb (C), Carl Zeiss Meditec (F), Eyenovia (C), Genentech (F), Heidelberg Engineering (F), National Eye Institute (F), Norvatis (C), Optos (F), Optovue (F), Sensimed (F), Topcon (F), Unity (C), Valeant (C)

References

1. Fantes FE, Anderson DR. Clinical histologic correlation of human peripapillary anatomy. *Ophthalmology*. 1989;96:20–25.
2. Jonas JB, Jonas SB, Jonas RA, et al. Histology of the parapapillary region in high myopia. *Am J Ophthalmol*. 2011;152:1021–1029.
3. Jonas JB, Jonas SB, Jonas RA, et al. Parapapillary atrophy: histological gamma zone and delta zone. *PLoS One*. 2012;7:e47237.
4. Cohen AI. Is there a potential defect in the blood-retinal barrier at the choroidal level of the optic nerve canal? *Invest Ophthalmol*. 1973;12:513–519.
5. Jonas JB, Konigsreuther KA, Naumann GO. Optic disc histomorphometry in normal eyes and eyes with secondary angle-closure glaucoma. II. Parapapillary region. *Graefes Arch Clin Exp Ophthalmol*. 1992;230:134–139.
6. Kim M, Kim T-W, Weinreb RN, Lee EJ. Differentiation of parapapillary atrophy using spectral-domain optical coherence tomography. *Ophthalmology*. 2013;120:1790–1797.
7. Dai Y, Jonas JB, Huang H, et al. Microstructure of parapapillary atrophy: beta zone and gamma zone. *Invest Opthalmol Vis Sci*. 2013;54:2013–2018.
8. Lee SH, Lee EJ, Kim T-W. Topographic correlation between juxtapapillary choroidal thickness and microstructure of parapapillary atrophy. *Ophthalmology*. 2016;123:1965–1973.
9. Kim YW, Lee EJ, Kim T-W, et al. Microstructure of β-zone parapapillary atrophy and rate of retinal nerve fiber layer thinning in primary open-angle glaucoma. *Ophthalmology*. 2014;121:1341–1349.
10. Yamada H, Akagi T, Nakanishi H, et al. Microstructure of peripapillary atrophy and subsequent visual field progression in treated primary open-angle glaucoma. *Ophthalmology*. 2016;123:542–551.
11. Akagi T, Iida Y, Nakanishi H, et al. Microvascular density in glaucomatous eyes with hemifield visual field defects: an optical coherence tomography angiography study. *Am J Ophthalmol*. 2016;168:237–249.
12. Suh MH, Zangwill LM, Manalastas PI, et al. Deep retinal layer microvasculature dropout detected by the optical coherence tomography angiography in glaucoma. *Ophthalmology*. 2016;123:2509–2018.
13. Jia Y, Wei E, Wang X, et al. Optical coherence tomography angiography of optic disc perfusion in glaucoma. *Ophthalmology*. 2014;121:1322–1332.
14. Wang X, Jiang C, Ko T, et al. Correlation between optic disc perfusion and glaucomatous severity in patients with open-angle glaucoma: an optical coherence tomography angiography study. *Graefes Arch Clin Exp Ophthal*. 2015;253:1557–1564.
15. Yarmohammadi A, Zangwill LM, Diniz-Filho A, et al. OCT angiography vessel density in healthy, glaucoma suspects, and glaucoma. *Invest Ophthalmol Vis Sci*. 2016;57:OCT451–OCT459.
16. Suh MH, Zangwill LM, Manalastas PI, et al. Optical coherence tomography angiography vessel density in glaucomatous eyes with focal lamina cribrosa defects. *Ophthalmology*. 2016;123:2309–2317.
17. Lee EJ, Kim TW, Lee SH, Kim JA. Underlying microstructure of parapapillary deep-layer capillary dropout identified by optical coherence tomography angiography. *Invest Ophthalmol Vis Sci*. 2017;58:1621–1627
18. Sample PA, Girkin CA, Zangwill LM, et al. The African Descent and Glaucoma Evaluation Study (ADAGES): design and baseline data. *Arch Ophthalmol*. 2009;127:1136–1145.
19. Chauhan BC, Burgoyne CF. From clinical examination of the optic disc to clinical assessment of the optic nerve head: a paradigm change. *Am J Ophthalmol*. 2013;156:218–227.e2.
20. Reis ASC, Sharpe GP, Yang H, et al. Optic disc margin anatomy in patients with glaucoma and normal controls with spectral domain optical coherence tomography. *Ophthalmology*. 2012;119:738–747.
21. Hodapp E, Parrish RK II, Anderson DR. *Clinical Decisions in Glaucoma*. St Louis: The CV Mosby Co.; 1993:52–61.
22. Jia Y, Tan O, Tokayer J, et al. Split-spectrum amplitude-decorrelation angiography with optical coherence tomography. *Opt Express*. 2012;20:4710–4725.
23. Jia Y, Morrison JC, Tokayer J, et al. Quantitative OCT angiography of optic nerve head blood flow. *Biomed Opt Express*. 2012;3:3127–3137.
24. Spaide RF, Fujimoto JG, Waheed NK. Image artifacts in optical coherence tomography angiography. *Retina*. 2015;35:2163–2180.
25. Mansouri K, Medeiros FA, Tatham AJ, et al. Evaluation of retinal and choroidal thickness by swept-source optical coherence tomography: repeatability and assessment of artifacts. *Am J Ophthalmol*. 2014;157:1022–1032.e3.
26. Zhang C, Tatham AJ, Medeiros FA, et al. Assessment of choroidal thickness in healthy and glaucomatous eyes using swept source optical coherence tomography. *PLoS One*. 2014;9:e109683.
27. Yasuno Y, Hong Y, Makita S, et al. In vivo high-contrast imaging of deep posterior eye by 1-microm swept source optical coherence tomography and scattering optical coherence angiography. *Opt Express*. 2007;15:6121–6139.
28. Kiumehr S, Park SC, Syril D, et al. In vivo evaluation of focal lamina cribrosa defects in glaucoma. *Arch Ophthalmol*. 2012;130:552–559.
29. Tatham AJ, Miki A, Weinreb RN, et al. Defects of the lamina cribrosa in eyes with localized retinal nerve fiber layer loss. *Ophthalmology*. 2014;121:110–118.

30. You JY, Park SC, Su D, et al. Focal lamina cribrosa defects associated with glaucomatous rim thinning and acquired pits. *JAMA Ophthalmol*. 2013;13:314–320.
31. Park SC, Hsu AT, Su D, et al. Factors associated with focal lamina cribrosa defects in glaucoma. *Invest Opthalmol Vis Sci*. 2013;54:8401–8407.
32. Faridi OS, Park SC, Kabadi R, et al. Effect of focal lamina cribrosa defect on glaucomatous visual field progression. *Ophthalmology*. 2014;121:1524–1530.
33. Lee EJ, Kim TW, Kim M, et al. Recent structural alteration of the peripheral lamina cribrosa near the location of disc hemorrhage in glaucoma. *Invest Ophthalmol Vis Sci*. 2014; 55:2805–2815.
34. Kim YK, Park KH. Lamina cribrosa defects in eyes with glaucomatous disc haemorrhage. *Acta Ophthalmol*. 2016;94: e468–e473.
35. Cohen J. Weighted kappa: nominal scale agreement with provision for scaled disagreement or partial credit. *Psychol Bull*. 1968;70:213–220.
36. Landis JR, Koch GG. An application of hierarchical kappa-type statistics in the assessment of majority agreement among multiple observers. Biometrics 1977;33:363–374.
37. Burgoyne CF. A biomechanical paradigm for axonal insult within the optic nerve head in aging and glaucoma. *Exp Eye Res*. 2011;93:120–132.
38. Langham M. The temporal relation between intraocular pressure and loss of vision in chronic simple glaucoma. *Glaucoma*. 1980;2:427–435.
39. Kim T-W, Kim M, Weinreb RN, et al. Optic disc change with incipient myopia of childhood. *Ophthalmology*. 2012;119: 21–26.e3.
40. Curcio CA, Saunders PL, Younger PW, Malek G. Peripapillary chorioretinal atrophy: Bruch's membrane changes and photoreceptor loss. *Ophthalmology*. 2000;107:334–343.
41. Strouthidis NG, Yang H, Reynaud JF, et al. Comparison of clinical and spectral domain optical coherence tomography optic disc margin anatomy. *Invest Ophthalmol Vis Sci*. 2009; 50:4709–4718.

Investigative Ophthalmology & Visual Science